

Title	The Effect of an Additional Alumina Layer in Improvement of Plasma Sprayed TBCs during High Temperature Applications
Author(s)	Afrasiabi, Abbas
Citation	Transactions of JWRI. 37(2) p57-p.61
Issue Date	2008-12
oaire:version	VoR
URL	https://hdl.handle.net/11094/12681
DOI	
rights	
Note	

Osaka University Knowledge Archive : OUKA

<https://ir.library.osaka-u.ac.jp/>

Osaka University

The Effect of an Additional Alumina Layer in Improvement of Plasma Sprayed TBCs during High Temperature Applications[†]

AFRASIABI Abbas^{*} and KOBAYASHI Akira^{**}

Abstract

Hot corrosion and bond coat oxidation are the main destructive factors in thermal barrier coatings (TBCs) and are the result of oxygen and molten salt penetration on the coating-gas interface. Hot corrosion and oxygen penetration behavior of two types of plasma sprayed TBCs were evaluated: a) usual YSZ (yttria stabilized zirconia), b) layer composite of YSZ/Al₂O₃ in which Al₂O₃ was as a top coat on a YSZ layer. Hot corrosion tests were carried out on the surface of coatings in molten salt (Na₂SO₄+V₂O₅) at 1050 °C for 40 h. The formation of monoclinic ZrO₂ and YVO₄ crystals as hot corrosion products caused the degradation of the mentioned TBCs. Oxidation tests were carried out on the coatings at 1100 °C for 22, 42 and 100 hours. Microstructure studies demonstrated the growth of TGO underneath the YSZ coating is higher than for YSZ/Al₂O₃ coating. Cracking was also observed in usual YSZ coating at the YSZ/ bond coat interface. So alumina coating as outer layer in YSZ/Al₂O₃ reduced the penetration of oxygen and molten salt into YSZ and resulted in the further resistance of TBC during high temperature application.

KEY WORDS: (Hot corrosion) (TBC) (Plasma spray) (YSZ/Al₂O₃) (Oxidation)

1. Introduction

Thermal barrier coatings are widely used in gas turbines to reduce thermal effect and increase turbine efficiency. The TBCs are usually composed of a MCrAlY bond coat (M=Ni,Co) as an oxidation resistant layer and yttria stabilized zirconia (YSZ) as a top coat that provides thermal insulation of the metallic substrate [1-6]. However there are shortcomings such as spallation, hot corrosion and phase transformation which reduce the durability of the coating [7-9]. Low quality fuels usually contain impurities such as Na and V which can form Na₂SO₄ and V₂O₅ salt on the surface of turbine blades. Such fused salts can react with yttria (the stabilizer component of YSZ) and cause transformation of tetragonal or cubic zirconia to the monoclinic phase during cooling [5,6]. This transformation is accompanied by 3-5% volume expansion, leading to cracking and spallation of TBCs [10,11].

Also application of TBC at high temperature causes the transfer of oxygen through the top coat towards the bond coat, so an oxidized scale can be formed on the bond coat which is termed the thermally grown oxide (TGO). Although this scale protects the substrate against

further oxidation, the growth of TGO during thermal cycling can lead to the failure of the YSZ layer [12-14].

Al₂O₃ material is more stable in chemical environment and considered as a oxygen barrier structure in comparison with zirconia. It seems that the use of fine alumina particles as a dense layer over YSZ coating can decrease oxygen diffusivity and salt penetration through this layer. Therefore, the aim of the present work is to reduce hot corrosion and suppress the growth of TGO thickness by alumina component.

In this regard, two types of plasma sprayed TBCs were prepared: the usual YSZ and a layer composite of (YSZ/Al₂O₃) in which Al₂O₃ was as a top coat over the YSZ layer. All of the layers were produced by plasma spray method which has many industrial applications and lower cost [3]. In this paper, the microstructure, chemical and phase analysis of the coatings were studied by SEM, EDS and XRD.

2. Experimental procedure

Nickel based superalloy (Inconel 738) disks of (ϕ 25 × 10 mm) which grit blasted with alumina particles

[†] Received on December, 26, 2008

^{*} Assistant Professor, Khorasan Science & Technology Park, Chemistry and Materials Department P.O. Box 91735-139, Mashhad, Iran

^{**} Associate Professor

Transactions of JWRI is published by Joining and Welding Research Institute, Osaka University, Ibaraki, Osaka 567-0047, Japan

were used as substrates. Three types of commercial powders were selected: Amdry 962 (Ni-22Cr-10Al-1Y, -106+52 μm) as bond coat, Metco 204 NS-G (ZrO_2 -8% Y_2O_3 , -106+11 μm) and Metco 105 NS (high purity Al_2O_3 , -53+15 μm) as TBC. Two types of coatings were produced by air plasma spray (APS) method which included: usual YSZ and layer composite of (YSZ/ Al_2O_3) in which Al_2O_3 was as a top coat on the surface of YSZ. **Table 1** indicates the characteristics of the coatings and the parameters of plasma spraying are listed in **Table 2**.

A mixture of 55 wt.% V_2O_5 and 45 wt.% Na_2SO_4 powders was selected as corrosive salt. The corrosive salt was spread over the surface of the coatings in a concentration of 30 mg/cm^2 . The specimens were set in an electric furnace with air atmosphere at 1050 $^\circ\text{C}$ for 40 hours and then cooled down inside the furnace. The coatings were inspected periodically after each of 8 h. For oxidation tests the as-sprayed coatings were put in an electric furnace with air atmosphere at 1100 $^\circ\text{C}$ for 22, 24 and 100 hours. All of the samples were sectioned with a diamond saw, cold epoxy mounted and fine polished. The microstructure and chemical composition of the coatings were examined by scanning electron microscopy (SEM, Cambridge, Cam Scan – MV 2300, U.K.) equipped with an energy dispersive spectrometer (EDS). X-ray diffraction (XRD) was used to determine the crystalline structure of the coatings.

3. Results and discussion

3.1. Oxidation

Figure 1 shows the cross sections of the two types of TBCs. In Fig. 1a, a usual TBC is observed which

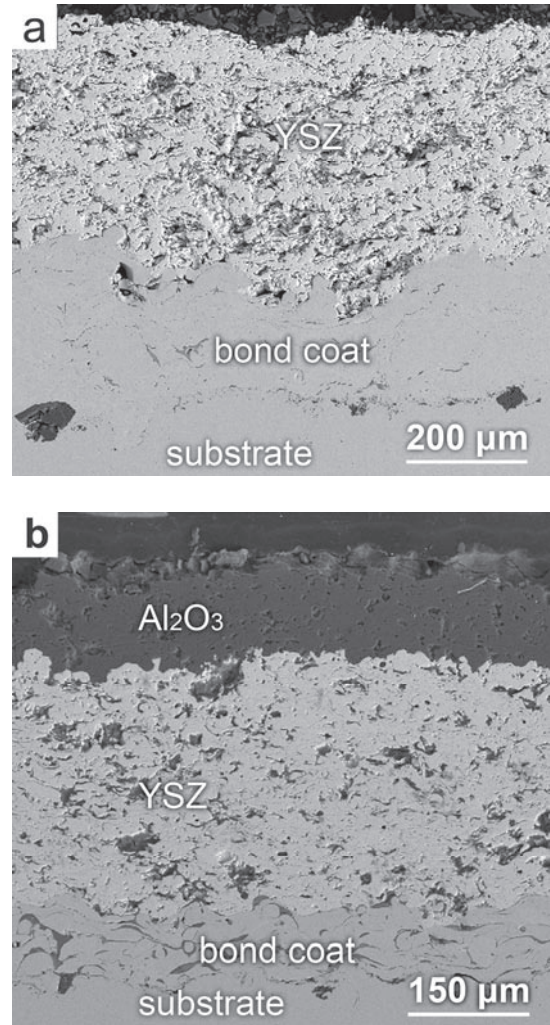


Fig. 1 Microstructure of the as sprayed coatings obtained by SEM: (a) YSZ ; (b) YSZ/ Al_2O_3 .

Table 1 Types of TBCs and thickness of layers (μm)

Type of TBC	NiCrAlY	YSZ*	Al_2O_3	Abbreviation
Usual YSZ	150	350	-	YSZ
Layer composite	150	250	100	YSZ/ Al_2O_3

YSZ* = yttria stabilized zirconia

Table 2 Parameters of plasma spraying

Parameter	NiCrAlY	YSZ	Al_2O_3
Current (A)	400	550	500
Voltage (V)	75	70	70
Primary gas, Ar (l/min)	57	38	38
Secondary gas, H_2 (l/min)	17	17	17
Powder feed rate (g/min)	45	35	30
Spray distance (cm)	15	7.5	7.5

includes bondcoat and YSZ layers. In Fig. 1b, the top coat is an Al_2O_3 layer and the YSZ coating is between the alumina layer and the bond coat. All of the coatings showed the lamellar structure which is a characteristic of plasma sprayed coatings.

Figures 2a and **2b** show the cross section of YSZ and YSZ/ Al_2O_3 coatings after 100 h oxidation at 1100 $^\circ\text{C}$. Oxygen penetrated through open porosities of the NiCrAlY layer, so oxide scales were formed within the bond coat. The comparison of Figs. 2a and 2b reveals the oxidized areas (dark zones) in the bond coat of YSZ are higher than in the bond coat of YSZ/ Al_2O_3 . The percentage of oxidized areas inside the bond coat was measured by image analysis giving 32 and 19% for YSZ and YSZ/ Al_2O_3 coatings, respectively. So it can be said that the internal oxidation of the bond coat for the YSZ/ Al_2O_3 was lower in comparison with the bond coat of the YSZ coating. In addition an oxide scale (TGO) was formed on the bond coat (**Figs. 3a** and **3b**), due to

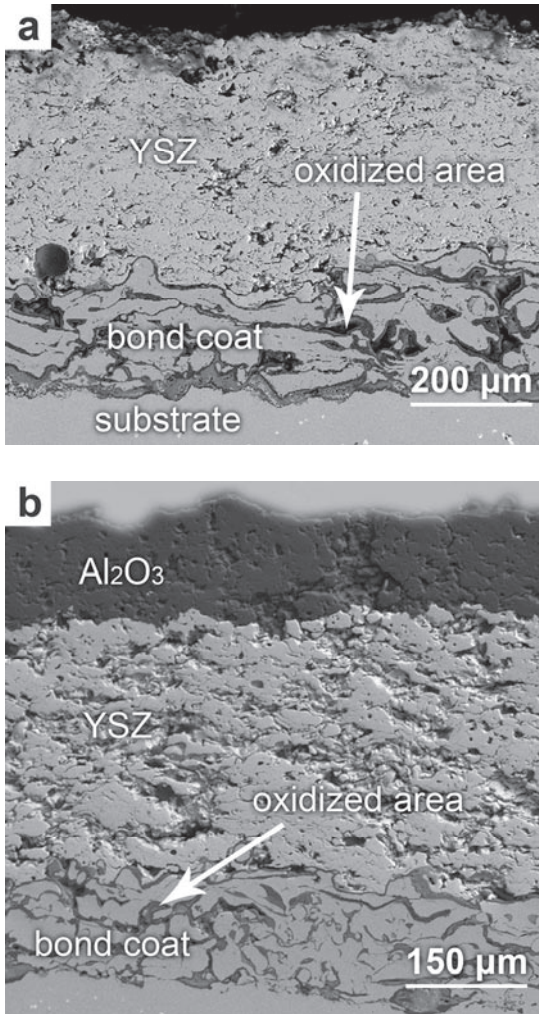


Fig. 2 SEM images showing the cross section of coatings after oxidation at 1100 °C for 100 h. (a) YSZ; (b) YSZ/Al₂O₃.

oxygen penetration through the ceramic layer. The examination of TGO by EDS exhibited a high percentage of Al and O, Thus the TGO comprises mainly Al₂O₃. As shown in Fig. 3a, crack formation occurred at the TGO/YSZ interface which belongs to the usual YSZ coating. The TGO usually comprises large residual compressive stresses when it cools to ambient temperature, because of its thermal expansion misfit with the substrate [3].

TGO thickness was measured along the bond coat/YSZ interface after oxidation at 1100 °C for 22, 42 and 100 h. The average of thickness for ten points was considered as the TGO thickness. **Figure 4** shows the TGO thickness versus time of oxidation for YSZ and YSZ/Al₂O₃ coatings. As shown in Fig. 4, the rate of TGO growth was fast during the first 22 h due to the inward penetration of O and outward diffusion of Al were rapid at these initial times. Then the Al₂O₃ layer was formed at the bond coat/YSZ interface and reduced the permeation

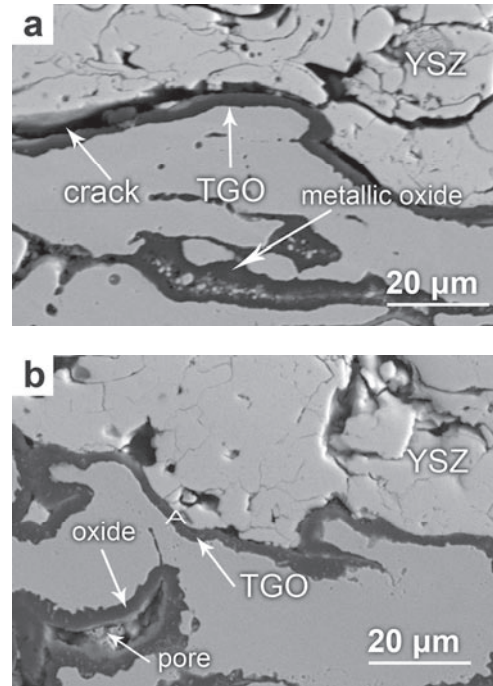


Fig. 3 Microstructure at the bond coat /ceramic layer interface after oxidation at 1100 °C for 100 h. (a) TGO in usual YSZ coating which includes cracks and delamination; (b) TGO in YSZ/Al₂O₃ coating, Al₂O₃ top coat has not been presented due to high magnification.

of oxygen toward bond coat, so the rate of TGO growth became slow after 22 h. Moreover, Fig. 4 reveals the rate of TGO growth in YSZ coating is higher than YSZ/Al₂O₃ coating which is accompanied with high tensile stress at the TGO/YSZ interface [15,16] and leads to the crack formation at the interface of the YSZ coating and the bond coat (Fig. 3a). These results indicate the existence of a dense alumina layer over the YSZ coating in TBCs reduces the oxygen penetration towards the bond coat.

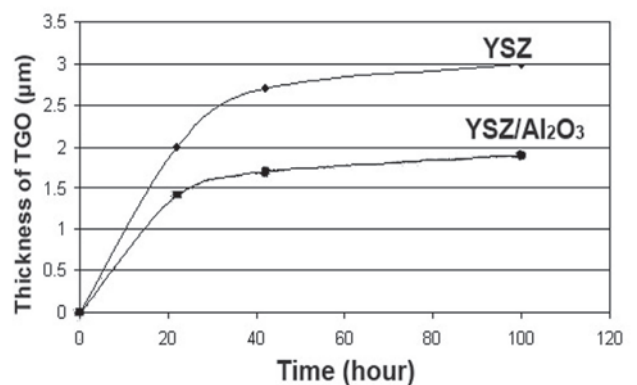


Fig. 4 The growth of TGO scale versus time of oxidation at 1100 °C for YSZ and YSZ/Al₂O₃ coatings.

Thus by using this method, the rate of TGO growth and detrimental oxides inside the bond coat decrease effectively and lead to less mechanical stresses and can cause the improvement of TBC life.

3.2. Hot corrosion

Figure 5 shows the SEM surface morphology of the coatings after 40 h of corrosion testing. Usual YSZ coating revealed a porous surface having some cracks and many crystals deposited on the surface (Fig. 5a). The alumina layer spalled at the YSZ/ Al_2O_3 interface, therefore Fig. 5b indicates the surface of YSZ as an inner layer. The shape of the crystals are rod type in the YSZ (Fig. 5a), and small rods with low number in the YSZ/ Al_2O_3 coating (Fig. 5b).

EDS analysis from the surface of the coatings (**Fig. 6**) demonstrated that the crystals were composed of yttrium, vanadium and oxygen, then they were identified by XRD analysis to be YVO_4 .

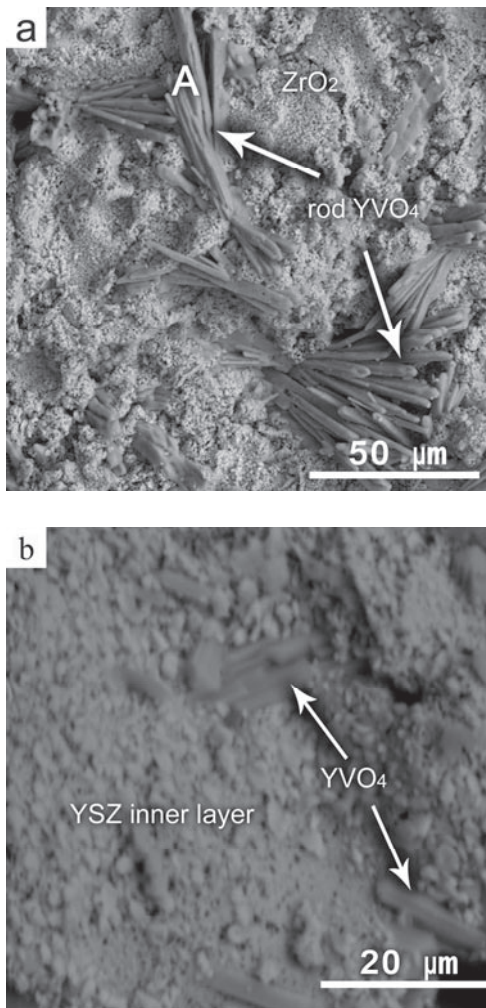


Fig.5 SEM micrographs of YVO_4 crystals on the surface of coatings after 40 h hot corrosion: (a) YSZ; (b) YSZ/ Al_2O_3 after spallation of Al_2O_3 layer.

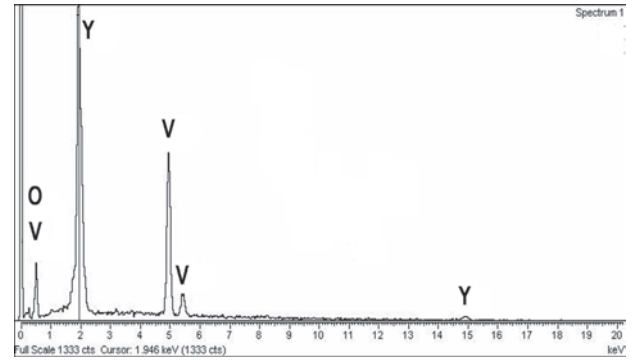


Fig. 6 EDS spectrum from the crystals on the surface of the coatings in Fig. 5.

The XRD analysis was performed on the surface of the coatings before and after hot corrosion. **Figure 7a** illustrates the XRD patterns of as-sprayed YSZ and YSZ/ Al_2O_3 TBCs that include the tetragonal phase of ZrO_2 , rhombohedral (α) and cubic (γ) phases of Al_2O_3 .

Figure 7b exhibits the XRD patterns of the coatings after hot corrosion tests. Monoclinic ZrO_2 and YVO_4 were formed on all of the coatings after exposure to molten salt at 1050 °C for 40 h, but the intensity of their peaks was different.

The comparison of XRD patterns after hot corrosion (Figs. 7a and 7b) shows the intensity of the main peak of YVO_4 is substantially higher in usual YSZ than YSZ/ Al_2O_3 . Thus, it can be said that the reaction rate of Y_2O_3 with molten salt considerably increased in the usual YSZ and decreased in the YSZ/ Al_2O_3 that was accompanied by the formation of remarkable amount of monoclinic phase in YSZ coating.

Although the YSZ/ Al_2O_3 coating showed spallation of the Al_2O_3 layer, but the YSZ as inner layer was without crack or delamination. So it can be said that formation of a small amount of monoclinic ZrO_2 at the YSZ/ Al_2O_3 interface led to the failure of Al_2O_3 layer.

The hot corrosion behavior and failure mechanism of TBCs in the present study comprises the following steps that are in agreement with previous investigations [17,18]:

- Molten salt penetration through microcracks and open porosities.
- Reaction of molten salt with the stabilizer of zirconia (Y_2O_3).
- Phase transformation of zirconia from tetragonal to monoclinic, due to the depletion of stabilizer which is accompanied by volume expansion of the coating.
- Formation of YVO_4 crystals with rod shape and average length of 40 μm in the usual YSZ coating that grow outward the surface and cause additional stresses in the coating (Fig. 5a).

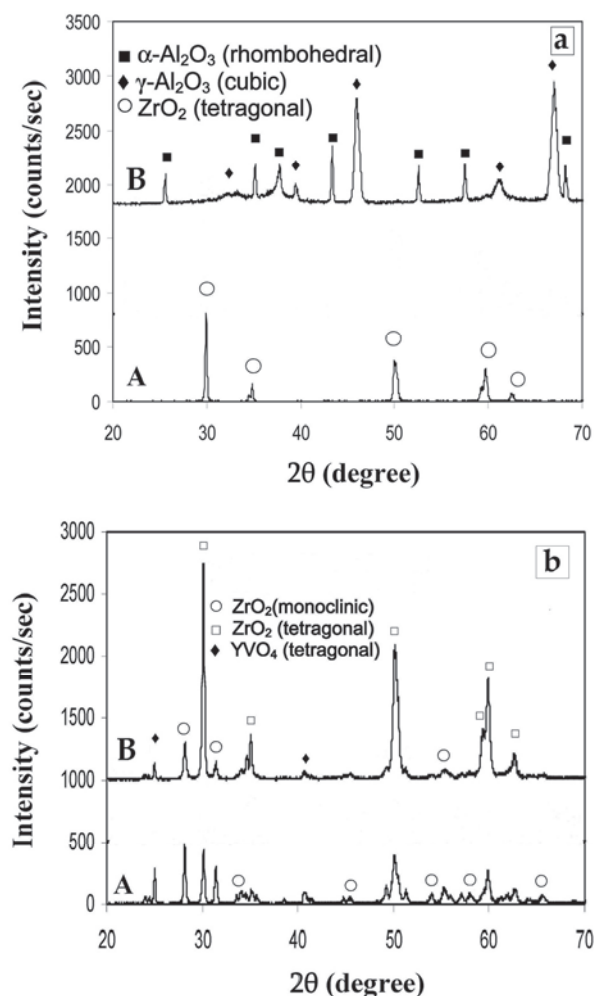


Fig. 7 XRD patterns from the surface of the coatings: (a) as sprayed TBCs, pattern A (YSZ); pattern B alumina layer of (YSZ/Al₂O₃); (b) after hot corrosion test, pattern A (YSZ); pattern B, YSZ layer of (YSZ/Al₂O₃).

So the protective and dense Al₂O₃ layer in YSZ/Al₂O₃ prevents the infiltration of molten salt into the YSZ layer and the removal of stabilizer (yttria) from this layer decreases substantially, hence the amount of monoclinic ZrO₂ and YVO₄ crystals are lower in YSZ/Al₂O₃ in comparison with YSZ coating. In addition, the rate of TGO growth and detrimental oxides inside the bond coat decreased effectively during high temperature oxidation which led to the less mechanical stresses. Thus the application of an additional alumina layer resulted in less destruction of YSZ and can cause the improvement of TBC life.

4. Conclusion

- (1) During oxidation of TBCs, the TGO layer was formed along the interface of bond coat and ceramic layer which includes mainly Al₂O₃.

- (2) The thickness of TGO in YSZ coating is higher in comparison with YSZ/Al₂O₃ coating after oxidation at 1100 °C for 100 h.
- (3) Although internal oxidation of the bond coat was severe for the usual YSZ coating, it decreased substantially for the bond coat of YSZ/Al₂O₃ coating due to lower oxygen ingress.
- (4) Hot corrosion of the YSZ coating was mainly due to reaction of molten salt containing V₂O₅ with Y₂O₃ which was then accompanied by formation of monoclinic ZrO₂ and YVO₄ crystals.
- (5) Monoclinic ZrO₂ and YVO₄ crystals led to the failure of TBCs.
- (6) In the YSZ/Al₂O₃ system, the presence of a dense Al₂O₃ top layer on YSZ reduced the infiltration of molten salt and resulted in the further resistance of TBC against hot corrosion.

References

- 1) H. D. Steffens, Kaczmark, *Welding in the World* 28 (1990) 224.
- 2) J.T. Demasi- Marcin, D.K. Gupta *Surf. Coat. Technol.* 68-69 (1994) 1.
- 3) A.G. Evans, D.R. Mumm, J.W. Hutchinson, G.H. Meier, F.S. Pettit, *Prog. Mater. Sci.* 46 (2001) 505.
- 4) J.R. Brandon, R. Taylor, *Surf. Coat. Technol.* 69 (10) (1992) 75.
- 5) I. Gurrappa, *J. Mater. Sci. Lett.* 17 (1998) 1267.
- 6) R.L. Jones, *J. Therm. Spray Technol.* 6(1) (1997) 77.
- 7) S. V. Joshi, M.P. Srivastava, *Surf. Coat. Technol.* 56 (1993) 215.
- 8) David W. Richerson, *Modern Ceramic Engineering*, by Marcel Dekker, 1999, P. 43 -45, 138-142.
- 9) Q. L. GE, T. C. LEI, J. F. MAO, Y. ZHOU, *J. Mater. Sci. Lett.* 12 (1993) 819.
- 10) M. P. Borom, C. A. Johnson, L. A. peluso, *Surf. Coat. Technol.* 87 - 89, (1996) 116.
- 11) C. Leyens, I. G. Wright, B. A. Pint, *Oxid. Met.* 54 (2000) 401.
- 12) D. R. Mumm, A. G. Evans, *Acta Mater.* 48 (2000) 1815.
- 13) U.Schulz, M. Menzebach, C. Leyens, Y. Q. Yang, *Surf. Coat. Technol.* 146 (2001) 117.
- 14) D. Strauss, G. Muller, G. Schumacher, et al. *Surf. Coat. Technol.* 135 (2001) 196.
- 15) J. S. Wang, A. G. Evans, *Acta Mater.* 47 (1999) 699.
- 16) A. G. Evans, J. W. Hutchinson, M.Y. He, *Acta Mater.* 47 (1999) 1513.
- 17) C. Batista, A. Portinha, R.M. Ribeiro, V. Teixeira, C.R. Oliveira, *Surf. Coat. Technol.* 200(2006) 6783.
- 18) Z. Chen, N. Q. Wu, J. Singh, S. X. Mao, *Thin Solid Films* 443 (2003) 46.